The lattice expansion in nanometre-sized Ni polycrystals

LETTER TO THE EDITOR

The lattice expansion in nanometre-sized Ni polycrystals

X D Liu†‡, H Y Zhang‡, K Lu†‡ and Z Q Hu‡

† International Centre for Materials Physics, Academia Sinica, Shenyang 110015, People's Republic of China
‡ State Key Laboratory of RSA, Institute of Metal Research, Academia Sinica, Shenyang 110015, People's Republic of China

Abstract. Solid Ni thin film samples with grain sizes of 6–15 nm were prepared by using a JG-PF high-frequency sputtering system. Quantitative x-ray diffraction measurements on the as-sputtered samples revealed that the peak positions of the x-ray diffraction lines of Ni nanocrystallites are lower than those of the corresponding perfect Ni crystal and that the deviation increases with a decrease in grain size. Further investigations showed that the lattice parameter of the Ni nanocrystallite is significantly increased by refining the grain size. The above results were qualitatively interpreted in terms of the thermodynamic theory, which suggests that a supersaturation of vacancies in the lattice structure of a nm-grained system is obtained as the grain size is decreased down to a few nanometres.

Investigations of the microstructure of nanocrystalline (NC) materials (Gleiter 1982, Birringer *et al* 1984) give rise to the question of whether or not the crystal structure remains perfect when the grain size of a polycrystal is refined down to a nanometre scale. Interestingly, Lu *et al* (1993) and our previous research (Liu *et al* 1993, 1994a, b) reveal that the lattice parameters of nanophases in nanocrystalline Ni–P and Fe–Cu–Si–B alloys synthesized by crystallization of the parent amorphous alloys deviate significantly from those of the perfect crystals. For example, in Ni_3P and Fe_2B nanophases, the lattice parameter is enlarged in the a-axis and is shortened in the c-axis simultaneously with the reduction of grain size. Very similar results were reported in a granular $Bi-(SiO_2)$ metal film produced by the magneto sputter deposition technique (Patterson *et al* 1992) and in NC Si materials synthesized by high-energy ball milling techniques (Gaffet and Harmelin 1991). It seems that the crystal structure of a nanocrystal is not perfect in comparison to its coarse-grained counterpart.

A JG-PF high-frequency ion beam sputtering system was utilized to prepare NC Ni film samples in this communication. The sputtering target used is a high-purity (>99.999%) Ni sample. The solid thin films (about 1 μm thick) were sputtered on a glass substrate (about 2.5 mm thick) in an ultrahigh-vacuum system. No oxidation was detected in the film sample using x-ray diffraction. A series of experimental Ni films with various grain sizes was obtained by modifying the sputtering conditions as shown in table 1. X-ray diffraction (XRD) experiments of the as-sputtered specimens were performed on a Rigaku x-ray diffractometer (D/MAX-8A, 12 kW, Cu Kα radiation). Monochromated x-rays with a carbon monochromator were employed in the present work.

Figure 1 gives a typical XRD spectrum of the as-sputtered Ni film sample. Only a crystalline Ni phase with an FCC structure can be indexed. The large width of reflections reveals the small size of the Ni polycrystals. The average grain size can be quantitatively determined from the XRD peak broadening by using the Scherrer equation after removing

Table 1. The sputtering conditions and grain sizes (d_{111}, d_{200} and d), as well as the peak positions of x-ray diffraction lines of the (111) and (200) planes of the experimental Ni samples.

Sample	A	B	C	D	E	F	G
V_b, (V)[a]	60	70	75	80	85	90	95
t_s, (min)	20	20	20	20	20	20	20
d_{111}, (nm)	5.6	7.1	7.8	7.3	7.7	10.6	15.8
d_{200}, (nm)	7.1	8.0	7.8	8.9	9.2	11.4	13.6
d (nm)	6.4	7.6	7.8	8.1	8.4	11.0	14.7
$2\theta_{(111)}$ (°)	44.031	44.230	44.265	44.271	44.290	44.351	44.382
$2\theta_{(200)}$ (°)	51.475	51.730	51.642	51.707	51.715	51.740	51.802

[a] Note: V_b refers to the negative bias voltage applied to the substrate of the sample; t_s refers to the sputtering time.
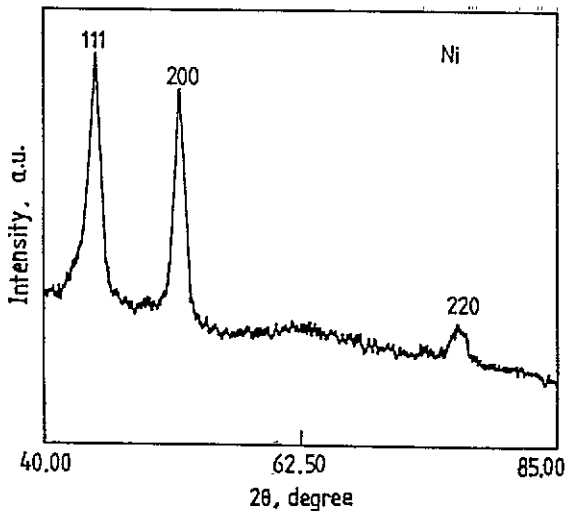
Figure 1. X-ray diffraction pattern of the as-sputtered Ni sample.

the instrumental broadening. The average grain sizes, d_{111} and d_{200}, calculated from (111) and (200) diffraction planes respectively are summarized in table 1. The 220 reflection peak in figure 1 was too weak to be used for the grain size determination. The mean value of d_{111} and d_{200} was taken as the average grain size of the as-sputtered samples as given in table 1. From table 1, a difference between d_{111} and d_{200} can be seen, indicating that the crystallites in the Ni samples are not equiaxed. Under the given experimental conditions, NC Ni films with average grain sizes of 6–15 nm were formed.

Figure 2 describes the XRD peaks of (a) (111) and (b) (200) of the tested samples. Table 1 lists the measured peak positions of (111) and (200) diffraction lines. It can be seen from figure 2 and table 1 that with decreasing grain size both diffraction peak angles, $2\theta_{(111)}$ and $2\theta_{(200)}$, shift to lower angles. In the case of sample A, $2\theta_{(111)}$ decreases by 0.351° compared to that of sample G. Pure Ni has an FCC structure and the lattice constant for the perfect Ni crystal is $a_0 = 0.35238$ nm as given in the ASTM card. The standard diffraction angles of the (111) and (200) lines are 44.50 and 51.84°, respectively. The data in table 1 therefore indicate that the diffraction angles of the (111) and (200) planes of the NC Ni samples deviate significantly from the ideal values of a perfect Ni crystal lattice though no
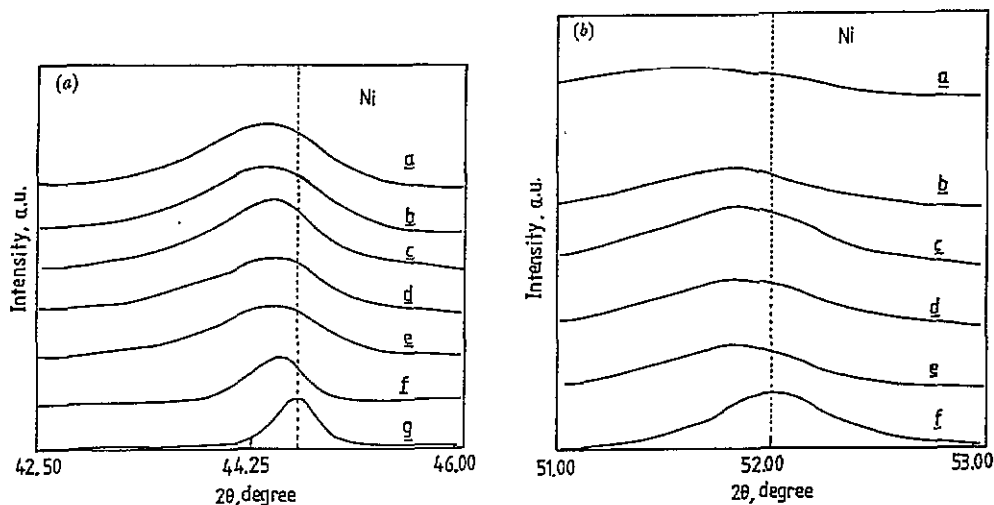
Figure 2. X-ray diffraction line broadening of the Ni film samples with various grain sizes for (a) the (111) plane, and (b) the (200) plane. Key: a, sample A; b, sample B; c, sample C; d, sample D; e, sample E; f, sample F; g, sample G.

solute atoms were introduced into the NC Ni films during the sputtering as indicated in the compositional analysis carried out using an electron microprobe. Also indicated is that the smaller the grain size the greater the deviation.

The lattice constant of the NC Ni samples was determined from the peak positions of the x-ray diffraction line broadening using Bragg's Law:

$$2d \sin \theta_{hkl} = \lambda. \tag{1}$$

Here, d is the interplanar spacing, θ_{hkl} is the diffraction angle of the (hkl) diffraction plane, λ is the x-ray wavelength. Reflections 111 and 200 were used to determine the lattice parameters. After the separation of $K\alpha_1$ and $K\alpha_2$, we took peak positions of $K\alpha_1$ of reflections of 111 and 200 as θ_{hkl} in equation (1) to calculate the lattice parameters. Table 2 describes the calculated results for the lattice constant of NC Ni samples. a_{111} and a_{200} are the lattice parameters calculated from the (111) and (200) diffraction planes, respectively. From table 2, one can see that both a_{111} and a_{200} increase rapidly with decreasing grain size and for the same sample $a_{111} > a_{200}$.

Table 2. Peak positions of x-ray diffraction lines, (111) and (200), and the change in lattice volume $(\Delta V/V_0)$ of the experimental Ni samples.

Sample	A	B	C	D	E	F	G
d (nm)	6.4	7.6	7.8	81.	8.4	11.0	14.7
a_{111} (nm) (± 0.00015)	0.35508	0.35419	0.35400	0.35414	0.35392	0.35343	0.35310
a_{200} (nm) (± 0.00013)	0.35475	0.35483	0.35352	0.35330	0.35310	0.35306	0.35295
$\Delta V_{111}/V_0$ (%)	2.32	1.55	1.38	1.50	1.32	0.90	0.61
$\Delta V_{200}/V_0$ (%)	2.03	2.10	0.97	0.78	0.61	0.58	0.49

We use $(a - a_0)/a_0$ to represent the deviation of the NC Ni lattice parameter from the equilibrium value, and give a plot of $(a - a_0)/a_0$ versus the reciprocal of the average grain size of the NC Ni samples in figure 3. Obviously, two straight lines were obtained for both a_{111} and a_{200} with a common reflexion point of $\bar{d} = 8.4$ nm when the average grain size decreases from 14.7 nm to 6.4 nm. The relative change in lattice parameters from the equilibrium value is from 0.16% up to 0.76%. For the smallest-grain-sized sample with $\bar{d} = 6.4$ nm, a_{111} and a_{200} depart from the ideal value by 0.76% and 0.67%, respectively.
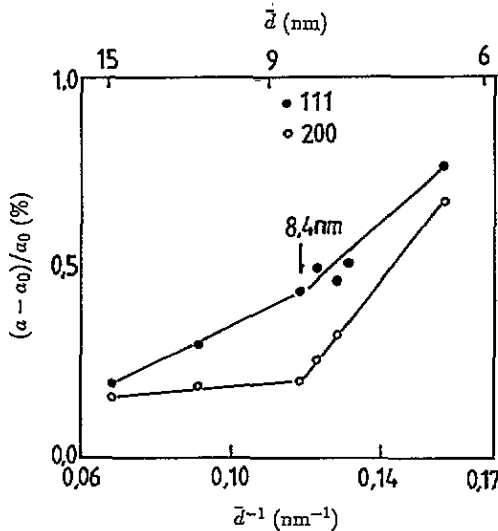

Figure 3. Variation of $(a - a_0)/a_0$ with the reciprocal of the average grain size of the NC Ni films.

Due to an enhanced lattice constant as in table 2 and figure 3, the volume of a unit cell of FCC Ni will be increased simultaneously. By using a similar method as that in figure 3, we introduce $\Delta V / V_0$ ($\Delta V = V - V_0$) to stand for the departure of the volume of a unit FCC Ni cell in the NC Ni sample from that of a perfect unit cell in the bulk Ni sample. The unit cell volume of the NC Ni sample was calculated using the a_{111} and a_{200} data, respectively. The calculated results are given in table 2. It is quite obvious from table 2 that the FCC Ni unit cell swells significantly with decreasing grain size. The volume of an FCC Ni unit cell in sample A is increased by about 2% in comparison to that of the perfect crystal lattice. In other words, there is a $\sim$2% excess volume in sample A.

From the above, it was found that the crystal structure of NC Ni samples had expanded relative to the perfect crystal structure. The smaller the grain size, the more serious the lattice expansion. The above observations suggest that the Ni lattice parameter is larger for smaller-grained nickel.

It was concluded by Lu *et al* (1993) from a thermodynamic consideration that the solubility of a solution will be increased significantly when the grain size is in the nanometre regime due to its higher energetic state, indicating that a supersaturated solution structure might be expected in nm-sized crystallites. The enhanced solubility can be expressed as the Gibbs–Thomson equation

$$C(T, d) = 4\Omega\gamma C_0/kTd \qquad (2)$$

where C_0 is the equilibrium solute stability in the coarse crystal, k is the Boltzmann constant, γ is the interfacial free energy, Ω is the atomic volume and d the grain size. In a pure system or in a stoichiometric intermetallic compound, the only possible 'solute atom' is either point defects or vacancies. Under these circumstances, a similar increase in the solubility of the point defects or vacancies in nm-crystallites can also be expected. In NC pure metal with a grain size of d, the equilibrium concentration of vacancies will be increased by

$$C^{v}(T, d) = 4\Omega\gamma \, \exp(S_f^{v}/k) \exp(-E_f^{v}kT)/kTd \tag{3}$$

where S_f^{v} and E_f^{v} are the formation entropy and formation energy for the vacancy, respectively.

From the above analyses, the departure from the perfect crystal lattice in a nm-grained system can be ascribed to a supersaturation of vacancies inside the nanocrystallites. The solution of vacancies in the crystal lattice will disturb the atomic arrangement around the vacancies to some extent, and ultimately results in an expanded lattice structure. The smaller the grain size, the higher the concentration of vacancies, i.e., the more significant will be the resultant lattice expansion. Since the variation of lattice constant with respect to $\bar{d}^{-1}$ does not completely obey a linear equation as in figure 3, it is suggested that the relation between $(a - a_0)/a_0$ and defect concentration is rather complicated, especially as the grain size is quite small. Further research is in progress.

To summarize, quantitative XRD studies on as-sputtered nanocrystalline Ni films with various grain sizes demonstrated that the crystal structure of the NC Ni films deviates significantly from that of the perfect Ni crystal, which is manifested by an expanded crystal structure. With decreasing grain size, the lattice expansion becomes more and more obvious from an increment of the lattice constant and an increase in the volume of an FCC Ni unit cell. The lattice expansion of nanophases can be qualitatively explained in terms of a supersaturation of vacancies inside the NC crystallites as a result of their higher energetic configurations.

References

Birringer R, Gleiter H, Klein H P and Marquardt P 1984 *Phys. Lett.* **102A** 365–7
Gaffet E and Harmelin M 1991 *J. Less-Common Met.* **157** 201–4
Gleiter H 1982 *Mater. Sci. Eng.* **52** 91–5
Liu X D, Lu K, Ding B Z and Hu Z Q 1994a *Chinese Sci. Bull.* (in Chinese) **39** 217–8
Liu X D, Lu K, Hu Z Q and Ding B Z 1993 *Nanostructured Mater.* **2** 581–6
Liu X D, Wang J T, Lu K, Zhu J and Jiang J 1994b *J. Phys. D: Appl. Phys.* **27** 165–8
Lu K and Sui M L 1993 *J. Mater. Sci. Technol.* **9** 419–22
Patterson B M, Unruh K M and Shah S I 1992 *Nanostructured Mater.* **1** 65–9